RSC Advances

PAPER

View Article Online
View Journal | View Issue

Cite this: *RSC Adv.*, 2018, **8**, 18880

Self-assembly of quaternary ammonium gemini surfactants in cyclohexane upon reinforcement by simple counterions†

Sheng-lu Deng, Jian-xi Zhao* and Zhi-xiu Wen

The quaternary ammonium gemini surfactants 12-*s*-12 (*s* = 2, 6, and 10) can produce homogeneous cyclohexane solutions with the assistance of salts, sodium benzoate (NaBez), sodium salicylate (NaSal), or sodium 2-bromoethanesulphonate (NaBres). In these samples, 12-*s*-12/salt formed aggregates and their structures were assigned by SAXS measurements together with POM observations. Among the three salts, both NaBez and NaBres had similar effects on assisting aggregate formation, but NaSal favoured the generation of aggregates of 12-*s*-12 with lower interface curvature. For example, both 12-2-12/NaBez and 12-2-12/NaBres formed an I_2 liquid crystalline (LC) phase with an *Fm*3*m* structure, but 12-2-12/NaSal generated a H_2 LC phase. Both 12-6-12/NaBez and 12-6-12/NaBres generated a H_2 LC phase, while 12-6-12/NaSal yielded both H_2 and V_2 phases with *Pn*3*m* symmetry, both of which co-existed in solution. The special effect of NaSal was attributed to its *ortho*-hydroxyl in the benzene ring. This favoured the formation of intermolecular hydrogen bonds among the NaSal molecules attracted to the quaternary ammonium head of 12-*s*-12. The water molecules joined between the NaSal molecules to build hydrogen-bonding bridges, which further increased the size of the 12-*s*-12 head. This benefited the formation of aggregates with lower surface curvature. In the systems of both NaBez and NaBres, the spacer length of the gemini surfactants dominated the morphology of the formed aggregates, wherein the effect of the salt was significantly weaker. Finally, the visco-elasticity of samples with similar aggregates was measured and the rheological behaviour discussed.

Received 29th March 2018
Accepted 3rd May 2018

DOI: 10.1039/c8ra02720j

rsc.li/rsc-advances

Introduction

Molecular self-assembly has become a major research topic in the past few decades. This is a spontaneous and reversible molecular associating process, during which intermolecular non-covalent forces such as aromatic ($\pi\cdots\pi$), hydrogen bonds, van der Waals, electrostatic and hydrophobic/solvophobic interactions are included.[1] At present, research on molecular self-assembly is very active and fruitful in biological,[2–6] materials,[7–10] and drug delivery[11–13] fields, which contributes to the development of these areas both in terms of scientific knowledge and practical application.

A surfactant is a small molecular amphiphile and its self-assembly is a classical and basic case in understanding intermolecular interactions. Among surfactants, a gemini molecule has a special chemical structure, which is made up of two hydrophilic head groups, two hydrophobic tails, and a spacer linked at, or near, the head-groups.[14,15] Such a molecular structure endows them with high surface activity and also dominates the morphology and structure of formed aggregates through altering the length of the spacer. Therefore, the study of gemini surfactants benefits the understanding of the mechanism of self-assembly and this topic has attracted much interest for decades.[15] Very recently, we reported the self-assembly of a class of typical cationic gemini surfactants, alkanediyl-α,ω-bis(dimethyldodecylammonium bromide), in cyclohexane.[16] The chemical structure of their molecules is shown in Scheme 1 and this class of gemini surfactants is abbreviated to 12-*s*-12, where 12 and *s* represents the number of carbon atoms in each alkyl tail and in the spacer chain, respectively.

Generally, 12-*s*-12 is insoluble in cyclohexane, and we used a newly-developed method to prepare homogeneous solutions of 12-*s*-12, namely, we added another equi-charged anionic surfactant, sodium hexanoate (SH) or sodium laurate (SL), to

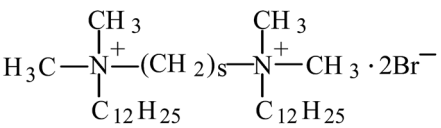

Scheme 1 Chemical structure of 12-*s*-12.

Institute of Colloid and Interface Chemistry, College of Chemistry and Chemical Engineering, Fuzhou University, Fuzhou, Fujian 350108, China. E-mail: jxzhao.colloid@fzu.edu.cn

† Electronic supplementary information (ESI) available. See DOI: 10.1039/c8ra02720j

neutralise the charge of 12-*s*-12.[16–18] Herein, these oppositely charged amphiphiles were figuratively referred to as helping surfactants. By way of this method, we obtained homogeneous solutions of 12-2-12/SH and 12-*s*-12/SL (including *s*4, *s*6, *s*8, and *s*10). The study showed that the spacer length of 12-*s*-12 strongly influenced their self-assembly, resulting in the formation of various aggregates: 12-2-12/SH, where the gemini had the shortest spacer in this series, formed an inverse micellar cubic liquid crystalline phase of *Fd*3*m* structure; 12-*s*-12/SL, including *s*4, *s*6, and *s*8, which contained an adequate length of spacer, formed an inverse hexagonal liquid crystalline phase packed by cylindrical assemblies of surfactants; 12-10-12/SL, in which the gemini had a longer spacer, formed dispersed reverse vesicles (in a lamellar structure).[16] Due to the difficulties associated with gemini surfactant dissolution in non-polar solvents, this was the first time that the effect of spacer length on complex aggregation in oil solution had been reported. Furthermore, we found that the addition of a helping surfactant can be replaced by the addition of a simple salt, by which a homogeneous solution was still obtained. Thus, further study of the self-assembly of 12-*s*-12 in cyclohexane upon reinforcement by added salts was warranted. We chose two aromatic salts, sodium benzoate (NaBez) and sodium salicylate (NaSal), as well as a simple salt, sodium 2-bromoethanesulphonate (NaBres), to assist in the production of 12-*s*-12 cyclohexane solutions. In the present work, typical *s*2, *s*6, and *s*10, which were respectively the shortest, intermediate, and longest, spacers of this gemini series, were used as representatives.

Results and discussion

Homogeneous solutions and their appearance

The preparation of solutions is described in the Experimental section, by which we obtained clear and homogeneous samples of equi-charged, mixed 12-*s*-12/salt. Some typical samples are shown in Fig. 1 at a fixed W_0, the molar ratio of water to gemini surfactant. Others are available in the ESI, as shown in Fig. S1, S3 and S7.† The range of W_0 allowed the formation of the homogeneous solutions as listed in Table 1: values outside this range of W_0 failed in this regard.

The added salts influenced the appearance of the solutions. For the three added salts, both 12-2-12 and 12-6-12 formed a gel and did not flow from an overturned vial. Although their appearance was similar, these systems had different aggregating structures and thus different rheological behaviours, as shown in the following sections. By way of comparison, 12-10-12 always maintained a flowable state, moreover, relying on the reinforcement effect of NaSal, an oily two-phase mixture was formed, where methyl orange dye was solubilised in the surfactant aggregates to distinguish between the two phases (Fig. 1: *s*10/NaSal at $W_0 = 50$). These results show the effects of both changing the spacer length and the added salt, which will be discussed below.

Aggregating structures

SAXS measurements were performed to assign the aggregate structures.

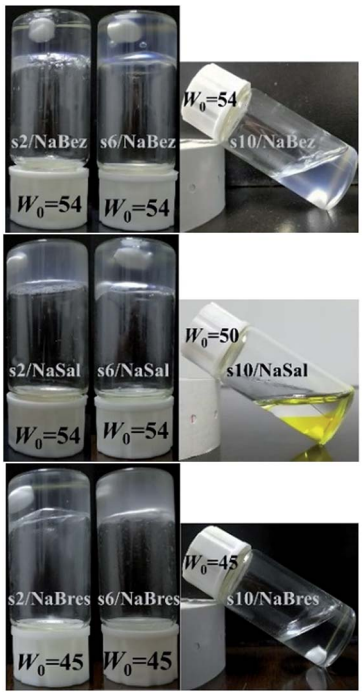

Fig. 1 Sample appearance of equi-charged mixtures of 12-*s*-12 (200 mmol L^{-1})/salt. In the sample of *s*10/NaSal at $W_0 = 50$, shown in the middle, an oily two-phase product was formed, where methyl orange dye was solubilised in the surfactant aggregates to indicate the two phases more clearly.

12-2-12/salt. Fig. 2 illustrates the SAXS spectra (plots of scattering intensity $I(q)$ *versus* scattering vector q) for 12-2-12/salt (200/400 mmol L^{-1}) in cyclohexane. For 12-2-12/NaBez at $W_0 = 54$, the SAXS pattern showed several resolved peaks (Fig. 2a), which indicated the existence of a liquid crystalline (LC) phase with long-range order.[19] Polarising micrograph (POM) observation did not reveal anything of significance and the image was covered in a dark background, indicating an isotropic sample. We inferred that the LC here should be of an I_2 phase, *i.e.*, reverse micellar cubic liquid crystalline.[20,21] Bragg reflections of 1 : 1.160 : 1.651 : 1.923 : 1.996 : 2.306 : 2.563 were obtained, which agreed with the characteristic ratios of $\sqrt{3} : \sqrt{4} : \sqrt{8} : \sqrt{11} : \sqrt{12} : \sqrt{16} : \sqrt{19} : \ldots$ (or 1 : 1.155 : 1.633 : 1.915 : 2 : 2.309 : 2.517 : …) of a face-centred close-packed (fcc) cubic structure of *Fm*3*m*.[22] These Bragg peaks can be indexed by the Miller indices *hkl* as shown in Fig. 2a.[22] For a cubic lattice with a cell lattice parameter a, the Bragg spacings are given by:

Table 1 The range of W_0 in the present three systems[a]

		NaBez	NaSal	NaBres
W_0 range	12-2-12	48–60	48–58	35–45
	12-6-12	48–60	48–60	35–45
	12-10-12	48–60	15–65	40–48

[a] W_0, the molar ratio of water to gemini surfactant.

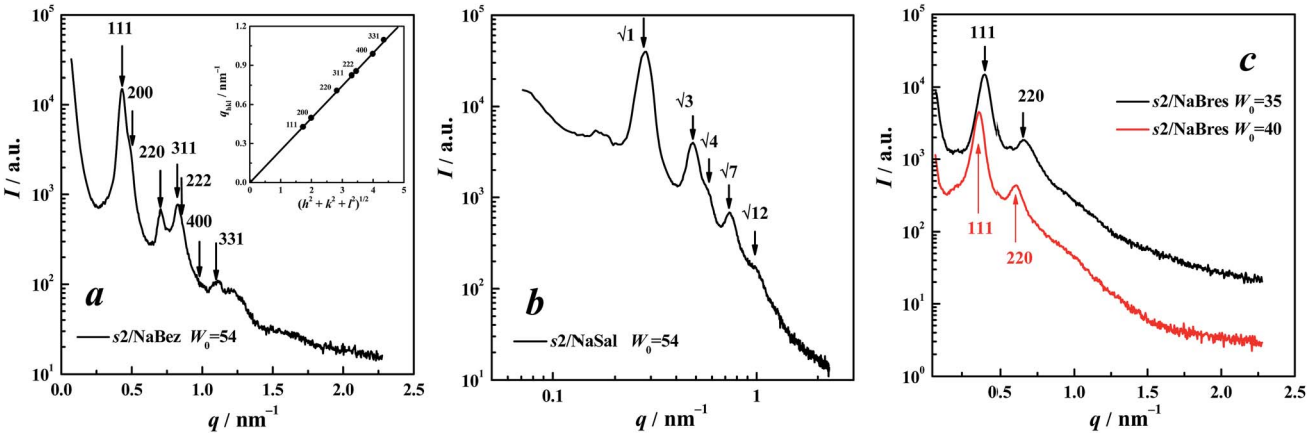

Fig. 2 SAXS spectra (plots of scattering intensity $I(q)$ *versus* scattering vector q) for 12-2-12/salt (200/400 mmol L^{-1}) in cyclohexane: (a) *s*2/NaBez at $W_0 = 54$, the inset denotes a plot of q for the reflections marked in the SAXS diffraction pattern *versus* $(h^2 + k^2 + l^2)^{1/2}$, (b) *s*2/NaSal, at $W_0 = 54$ and (c) *s*2/NaBres at $W_0 = 35$ and 40, repectively.

$$q_{hkl} = \frac{2\pi\sqrt{h^2 + k^2 + l^2}}{a} \quad (1)$$

The inset in Fig. 2a shows the experimental values of q_{hkl} as a function of $(h^2 + k^2 + l^2)^{1/2}$, in which the data are fitted using a straight line passing through the origin, for which the regression coefficient R^2 is 0.9999. Moreover, the most intense (111) reflection shown in Fig. 2a agrees with the featured *Fm*3*m* space group.[20] All these facets supported the assignment of *Fm*3*m* symmetry.

Comparatively speaking, another symmetrical structure, *Fd*3*m*, which is a tetrahedrally close-packed (tcp) form,[7] was more frequently encountered in reverse micellar systems;[19,23–27] however, such a matching style was thought to be impossible in the present case because the strongest (the first) peak did not correspond to the most intense (311) reflection of *Fd*3*m*.[20] Although *Fm*3*m* packing is rarely encountered, it has been reported in a previous paper focussing on systems containing phosphatidychline/water/organic solvents (cyclohexane, limonene, or isooctane).[22] Very recently, we also assigned this structure in the cyclohexane system of anionic surfactant, sodium dodecyl sulphate (SDS), together with an aliphatic salt, tetraalkylammonium bromide (TAABr). This situation of a lack of *Fm*3*m* is probably due to too few cases of surfactants being tested in non-polar solvents because of the difficulty of dissolving them. This symmetrical structure should be also common if more oil-homogeneous systems of surfactants can be achieved.

Fig. 2b shows the SAXS spectrum of 12-2-12/NaSal (200/400 mmol L^{-1}) in cyclohexane at $W_0 = 54$. The reflection peak positions had a ratio of 1 : 1.713 : 2.024 : 2.648 : 3.482, which obeyed the characteristic relationship of 1 : √3 : 2 : √7 : √12 : … (or 1 : 1.732 : 2 : 2.646 : 3 : 3.464 : …) of a hexagonal symmetrical H_2 structure (*i.e.*, the hexagonal arrangement of inverted cylindrical assemblies of surfactants).[24,25] POM observation also showed typical textures of the hexagonal LC phase (Fig. 3a).[21,28,29] These all contributed to the 12-2-12/NaSal forming a H_2 phase.

Compared with the two aforementioned aromatic counterions, benzoate and salicylate, 2-bromoethanesulphonate is small; moreover, the polarised image of the 2-2-12//NaBres sample was also covered in a dark background. Thus, we again inferred its aggregating structures to be an I_2 phase. In the SAXS spectra at $W_0 = 35$ and 40 respectively(Fig. 2c), two resolved peaks were observed, indicating LC samples.[19] The ratio of the two peaks was 1 : 1.637 at $W_0 = 35$ and 1 : 1.639 at $W_0 = 40$, respectively, obeying the characteristic ratio of √3 (111) : √8 (220) (or 1 : 1.633) of *Fm*3*m* symmetry.[22] Compared with the reflections of 12-2-12/NaBez (Fig. 2a), here the (200) reflection was not observed. Perhaps this was reasonable because the (200) reflection of the *Fm*3*m* phase is indeed often missed, as pointed out by Hamley *et al.*[30] and Martiel *et al.*[22] Therefore, an *Fm*3*m* symmetrical array was assigned to the structure of the 12-2-12//NaBres aggregation.

As seen above, both 12-2-12/NaBez and 12-2-12/NaBres yielded the cubic LC phase with *Fm*3*m* symmetry, while 12-2-12/NaSal led to the formation of a hexagonal H_2 phase. This phenomenon, *i.e.* the effect of both NaBez and NaBres being similar while that of NaSal differed, also occurred in the cases of 12-6-12 and 12-10-12, as discussed below.

12-6-12/salt. The spacer of 12-6-12 contains six carbon atoms and its stretched length reaches 0.889 nm as calculated by d_s/(nm) = 0.127(s + 1),[31] which is significantly longer than that (0.381 nm) of 12-2-12. This length (0.889 nm) is close to the electrostatic equilibrium distance between the two head-groups of dodecyltrimethylammonium bromide (C_{12}TABr), which corresponds to the monomer surfactant of the 12-*s*-12 series, packed on the micelle, which was estimated to be *ca.* 0.9 nm long.[31] Thus, 12-6-12 can be considered as a simple dimer of its monomer surfactant and therefore it becomes a representative of the gemini structure of this series.

Fig. 4a shows the SAXS spectrum for 12-6-12/NaBez (200/400 mmol L^{-1}) in cyclohexane at $W_0 = 54$. The reflection position ratio was found to be 1 : 1.733 : 1.990 : 2.648 : 3.009 : 3.466, corresponding to the characteristic ratio of 1 : √3 : √4 : √7 : √9 : √12 : … (or 1 : 1.732 : 2 : 2.646 : 3 : 3.464 : …) of the H_2 phase.[24,25] POM

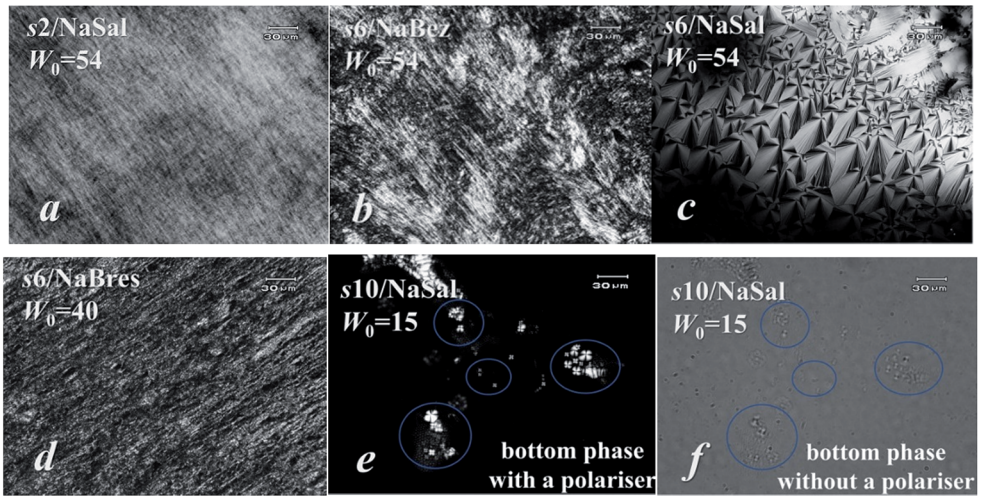

Fig. 3 Polarising micrographs of equi-charged mixtures of 12-2-12/NaSal (a), 12-6-12/NaBez (b), 12-6-12/NaSal (c), and 12-6-12/NaBres (d) (200/400 mmol L^{-1}), as well as micrographs of the bottom phase of 12-10-12/NaSal (200/400 mmol L^{-1}) at $W_0 = 15$ with (e) and without (f) a polariser.

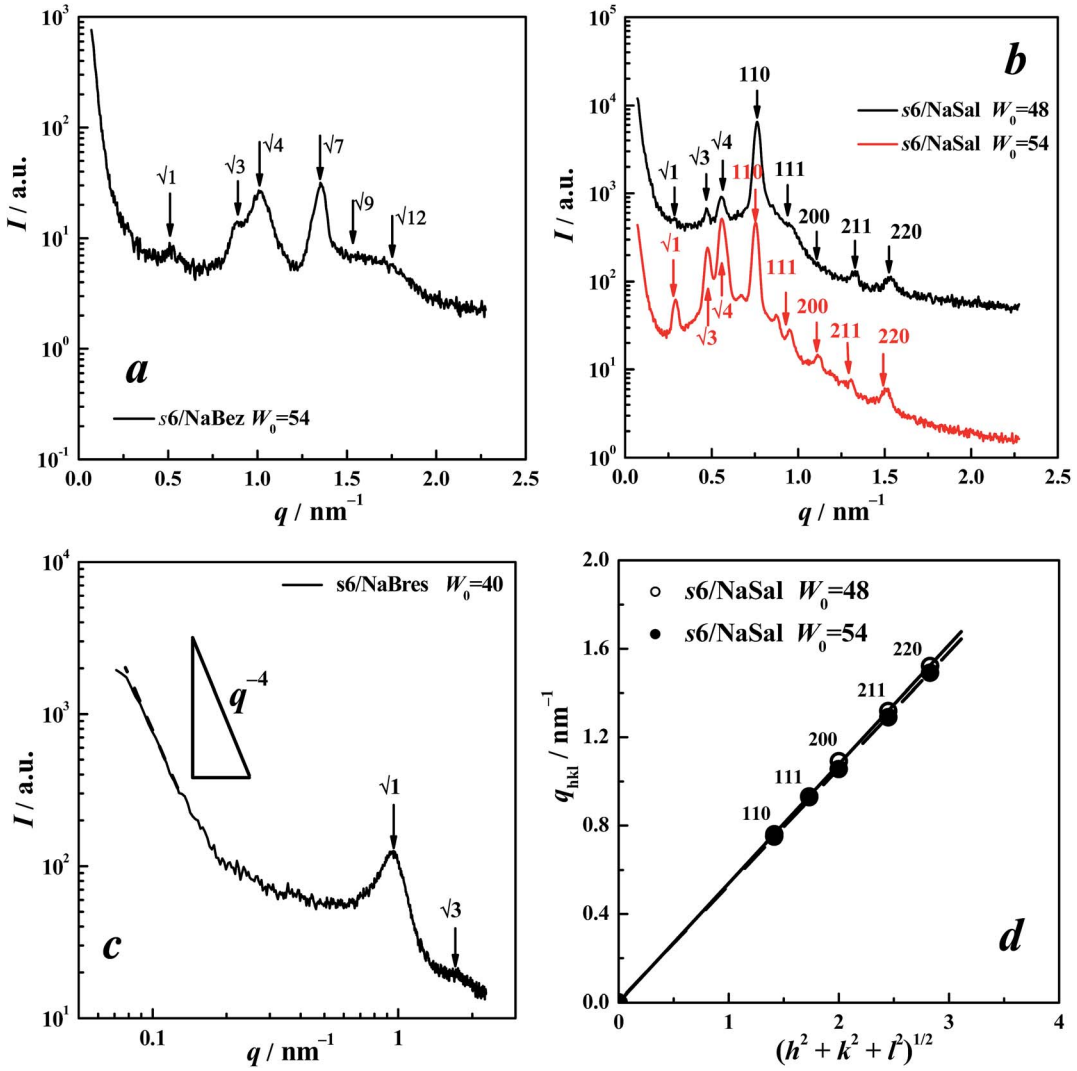

Fig. 4 SAXS spectra for 12-6-12/salt (200/400 mmol L^{-1}) in cyclohexane: (a) *s*6/NaBez, (b) *s*6/NaSal, and (c) *s*6/NaBres. The plots of *q versus* $(h^2 + k^2 + l^2)^{1/2}$ for the *Pn*3*m* structure of *s*6/NaSal are shown in (d).

observation also showed typical textures of a hexagonal structure (Fig. 3b),[21,28,29] supporting the postulated formation of a H_2 phase in this sample.

The SAXS diffraction patterns for 12-6-12/NaSal (200/400 mmol L^{-1}) in cyclohexane at $W_0 = 48$ and 54 are shown in Fig. 4b. The reflections were distinguished into two groups: one group contained the first three peaks, and another group contained the other peaks. For the first three peaks, the position ratio was 1 : 1.713 : 2.01 for $W_0 = 48$ and 1 : 1.721 : 2 for $W_0 = 54$, which obeyed the characteristic relationship of $1 : \sqrt{3} : 2 : \ldots$ (or 1 : 1.732 : 2 : …) of the hexagonal H_2 structure.[24,25] For the second group, the positions were in the ratio of 1 : 1.226 : 1.435 : 1.736 : 2.001 for $W_0 = 48$ and 1 : 1.248 : 1.419 : 1.736 : 2.005 for $W_0 = 54$. These correspond to the characteristic reflection ratio of $\sqrt{2} : \sqrt{3} : \sqrt{4} : \sqrt{6} : \sqrt{8} : \ldots$ (or 1 : 1.223 : 1.414 : 1.732 : 2 : …) of the bi-continuous cubic structure *Pn3m* (V_2 phase).[24] The plots of experimental q_{hkl} *versus* $(h^2 + k^2 + l^2)^{1/2}$ are shown in Fig. 4d, where the data were fitted by a straight line passing through the origin, for which the regression coefficients R^2 all reached 0.9999. Moreover, the strongest experimental peak corresponded to the most intense (110) reflection of *Pn3m* symmetry.[24] These supported the evidence suggesting the presence of a *Pn3m* structure in this system.

In general, bi-continuous cubic phases can be assigned to one of three space groups, *Ia3d*, *Pn3m* or *Im3m*, regardless of whether or not they are normal or inverted aggregations.[24,25,32] Among these, *Ia3d* is the most common, but its (211) reflection is the most intense, rather than the (110) reflection as shown in Fig. 4b. This eliminates the possibility of *Ia3d* symmetry from the present structure. Although the *Im3m* structure also yields the most intense reflection from its (110) plane, its characteristic reflection ratio is $\sqrt{2} : \sqrt{4} : \sqrt{6} : \sqrt{8} : \sqrt{10} : \sqrt{12} : \ldots$, not agreeing with the present data as revealed in Fig. 4b, thus this structure was also eliminated. Finally, in the system of 12-6-12/NaSal, the two phases H_2 and V_2 (*Pn3m* structure) co-existed and were duly assigned. In fact, this phenomenon of LC multiphase co-existence has also been observed elsewhere. For example, L–H, L–L_α, and H–L_α co-existed in different areas of the phase diagram of an alkylbenzene sulphonate (LAS)/alkyl ethoxysulphates (AES)/H_2O system,[33] and cubic V_2 phases, with *Im3m* and *Ia3d* structures, were also found to co-exist in Brij-type nonionic surfactant/IPM-PEG 400/H_2O systems.[34]

For 12-6-12/NaBres, Fig. 4c shows the SAXS spectrum, where scattering in the low-q region showed characteristic q^{-4} dependency as marked by solid lines. This was indicative of sharp interfaces,[35–37] suggesting that a LC phase was present in the sample: however, the present Bragg reflections were atypical and only two peaks can be distinguished. A position ratio of 1 : 1.738 was obtained, indicating that the LC phase here was a H_2 phase.[24,25] The POM data shown in Fig. 3d supported this assignment.

Similar to the case of 12-2-12/salt, both NaBez and NaBres caused similar effects on 12-6-12, all yielding a H_2 phase, but NaSal induced relatively complex forms of aggregation, where H_2 and V_2 (*Pn3m* structure) phases were found to co-exist in the samples. Comparatively speaking, the surface curvature of the aggregates in the V_2 phase is lower than that in the H_2 phase:[24,25] this meant that NaSal can induce the formation of aggregates with lower surface curvature in comparison to NaBez and NaBres, which agrees with the results obtained in the case of 12-2-12/salt.

12-10-12/salt. The spacer in 12-10-12 was the longest among the three representative gemini surfactants. The SAXS spectra of 12-10-12/salt are shown in Fig. 5, in which the structure of 12-10-12/NaSal aggregates formed in the bottom of the oily two-phase product should be easily assigned. In Fig. 5b, the slope in the low-q region was −2, which is generally indicative of the presence of a lamellar phase.[38] This feature, together with the POM data shown in Fig. 3e, where clear bright crosses are observed, suggested a lamellar structure was present in the sample.[38–41] Furthermore, a micrograph recorded without polarisers showed separated, spherical aggregates (Fig. 3f). This indicated that the lamellar structure characterised by SAXS, and its polarised texture should be dispersed. Thus, reverse vesicles can be assigned as the form of this sample.[41]

In both Fig. 5a and c, similar SAXS patterns were obtained, which were analogous to the results yielded in the cases of 12-2-

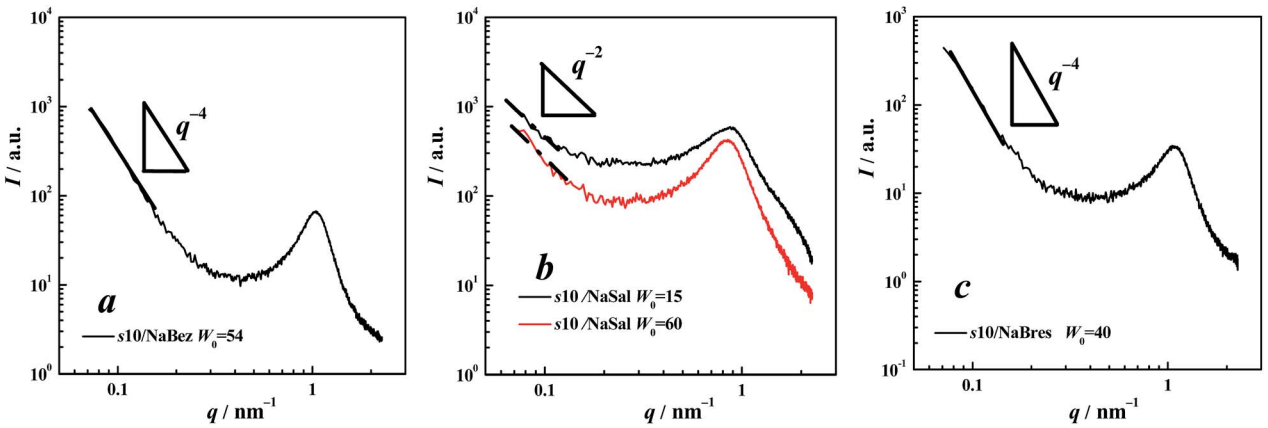

Fig. 5 SAXS spectra for 12-10-12/salt (200/400 mmol L^{-1}) in cyclohexane: (a) *s*10/NaBez, (b) *s*10/NaSal (bottom-phase), and (c) *s*10/NaBres.

12 and 12-6-12, where both NaBez and NaBres induced the same effect on the gemini surfactants. For the cases of 12-10-12/NaBez and 12-10-12/NaBres, a liquid crystalline phase should exist due to q^{-4} dependency in the low-q region. POM observations revealed nothing of significance and the image was covered in a dark background, corresponding to the formation of an isotropic micellar cubic phase, or a bi-continuous cubic phase. According to this regularity, *i.e.*, the surface curvature of the aggregates induced by NaBez or NaBres was always higher than that induced by NaSal, we can assume that both 12-10-12/NaBez and 12-10-12/NaBres formed a V_2 phase, which either satisfied the changing sequence of the aggregating phase from $L_\alpha \rightarrow V_2 \rightarrow H_2 \rightarrow I_2 \rightarrow L_2$ when increasing the surface curvature of the aggregate,[24,25] or agreed with the POM observations for this sample. However, further assignment was difficult because only one Bragg reflection was obtained.

Discussion of the effects of the salt and the gemini spacer length

The salt-reinforced aggregate structures of 12-*s*-12 are summarised in Table 2, in which both NaBez and NaBres showed similar effects on assisting with 12-*s*-12 aggregation, but NaSal induced 12-*s*-12 to form aggregates with lower surface curvature than those influenced by NaBez and NaBres. This can be generally interpreted in terms of the increased surfactant head size being caused by the additive that interacts with the head-group of the surfactant.[42] In the present systems, the counterions were all attracted to the quaternary ammonium head-groups of 12-*s*-12 through electrostatic interaction and thus increased the head size depending on the volume of the counterion present. NaBres has a relatively small volume compared to that of both NaBez and NaSal, while the latter two are similar in size[43] because NaSal (sodium 2-hydroxybenzoate) has only one more *ortho*-hydroxyl in its chemical structure than NaBez (sodium benzoate). However, it was just this one hydroxyl that induced a special effect of NaSal different from that of NaBez. It is known that the hydroxyl of NaSal formed an intramolecular hydrogen-bond with its carboxyl group when NaSal existed individually in the solution.[44,45] When a cationic surfactant was added to the solution, electrostatic interactions occurred between the cationic head-group of the surfactant and the Sal^- ion, which weakened the intramolecular hydrogen bonding of NaSal and yielded a dominance of the intermolecular hydrogen bonding among NaSal molecules.[46] For an inverted aggregation system, another important factor in increasing the size of the surfactant head that cannot be ignored is the role of the added trace amount of water. As revealed by Shchipunov *et al.* in realising the formation of reverse wormlike micelles by lecithin,[47,48] the added water molecules are thought to bridge the hydroxyl groups of neighbouring lecithin molecules, resulting in a significant increase in the size of the lecithin head and thus the formation of reverse worms. This mechanism was also thought to be in the present in the case of NaSal, *i.e.*, several water molecules joined between the NaSal molecules to build hydrogen-bonding bridges, which linked both themselves and the neighbouring NaSal molecules. All these factors greatly increased the effective size of the head region of 12-*s*-12, including the quaternary ammonium ions themselves, the Sal^- ions, and the bridged water molecules. As a result, the increase in the effective size of the 12-*s*-12 head must be significantly larger than that induced by NaBez, and the special effect of NaSal was therefore created. A schematic description of the mechanism underpinning this behaviour is shown in Fig. 6.

IR measurements provided evidence supporting this mechanism. Herein, 12-6-12 was chosen as a representative of the gemini surfactants. As seen from Fig. 7, the IR spectrum of single NaSal showed characteristic bands both at 3434 cm^{-1} and between 2400–2700 cm^{-1}, the former has been assigned to the hydroxyl group in an associated state[49] and the latter was indicative of the intramolecular hydrogen bonding between C=O and the OH group.[50] For the solid of the equi-charged *s*6/NaSal mixture, the large broadening bands between 2400–2700 cm^{-1} disappeared and only the 3434 cm^{-1} band was retained, which demonstrated the dominance of intermolecular hydrogen bonding among the NaSal molecules. When equi-charged *s*6/NaSal was dissolved in DMSO, and no water was added, its IR spectrum also only showed the band at 3434 cm^{-1}. As a trace amount of water was added ($W_0 = 48$), *s*6/NaSal formed aggregates in cyclohexane as discussed in Section 3.2 and its characteristic band appeared at 3386 cm^{-1}, indicating a frequency shift from 3434 cm^{-1} (without water) to 3386 cm^{-1} (with water). The frequency decrease of 48 cm^{-1} was comparable with that reported by Shchipunov *et al.*,[47] by which they suggested the mechanism of water molecules bridging neighbouring lecithin molecules through hydrogen bonds. Accordingly, we believe a similar mechanism also acts in the present case.

For a gemini surfactant system without a salt, the length of the spacer chain dominates the size of the head, as found in our previous work.[16] The result of 12-*s*-12/SL(SH) association in cyclohexane is shown in the last row of Table 2. A similar effect

Table 2 Formed aggregating mesophases

	Aggregating mesophase			
	NaBez	NaSal	NaBres	SH or SL^3
12-2-12	I_2 (*Fm*3*m*)	H_2	I_2 (*Fm*3*m*)	I_2 (*Fd*3*m*)
12-6-12	H_2	H_2 and V_2 (*Pn*3*m*)	H_2	H_2
12-10-12	V_2	Reverse vesicles	V_2	Reverse vesicles

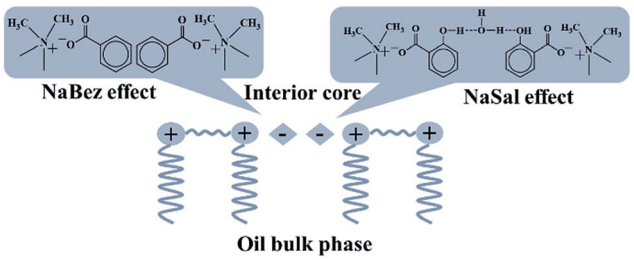

Fig. 6 Schematic of the mechanism of the NaSal effect on 12-*s*-12 aggregation in cyclohexane.

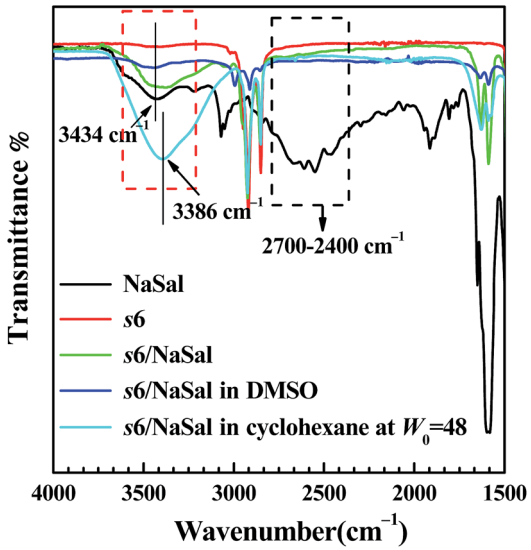

Fig. 7 FT-IR spectra of the 12-*s*-12/NaSal system.

of the 12-*s*-12 spacer in the present salt-containing systems can also be found in Table 2, where different structures corresponded to respective spacers at a fixed salt. At fixed NaBez or NaBres, the length of the spacer determined the associating structure of 12-*s*-12, which indicated that it is a controlling factor when only a simple salt was added. For NaSal, which conferred a special effect helping to increase surfactant head size as discussed above, the situation is more complicated: it not only induced the formation of surfactant aggregates with lower surface curvature but also may allow the co-existence of multi-type aggregates.

Visco-elastic properties

In this section, we compared the visco-elastic properties of the samples with similar aggregates.

12-2-12/NaBez and 12-2-12/NaBres. 12-2-12/NaBez and 12-2-12/NaBres both formed an I_2 phase with a *Fm*3*m* structure. Fig. 8 shows oscillatory sweep rheograms of 12-2-12/NaBez and 12-2-12/NaBres, which had the characteristics of a Maxwell fluid, *i.e.*, after crossing, the elastic modulus (G') gradually increased and the viscous modulus (G'') decreased with increasing frequency, ω. This agrees with general observations made of cubic liquid crystalline systems, where Maxwell fluid behaviour was often encountered.[51] In the present systems, the crosses lay at low frequencies of 0.015 to 0.025 rad s^{-1}. This resulted in a long relaxation time, τ_R, which is estimated as $1/\omega_C$, where ω_C is the frequency of crossing.[52,53] This was probably due to the presence of the I_2 phase in the present systems rather than the V_2 phase.[51] The elastic plateau modulus, G'_P, *i.e.* the value of G' at the high-frequency limit, can be obtained using the method suggested by Wu *et al.*[54,55] The G'_P values of 12-2-12/NaBez were one order of magnitude larger than that of 12-2-12/NaBres.

12-6-12/NaBez and 12-6-12/NaBres. 12-6-12/NaBez and 12-6-12/NaBres both formed a H_2 phase. Similar to cubic liquid crystalline systems, hexagonal liquid crystalline samples also follow Maxwell fluid behaviour, but not as perfectly over the

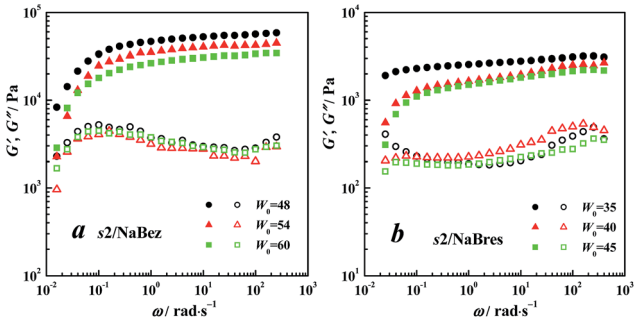

Fig. 8 Oscillatory sweep rheograms of 12-2-12/NaBez (a) and NaBres (b) (200/400 mmol L^{-1}) in cyclohexane, where solid and open symbols represent G' and G'', respectively.

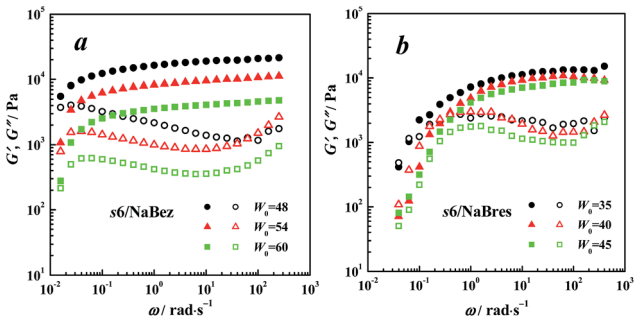

Fig. 9 Oscillatory sweep rheograms of 12-6-12/NaBez (a) and NaBres (b) (200/400 mmol L^{-1}) in cyclohexane, where solid and open symbols represent G' and G'', respectively.

range of frequencies tested due to the complexity of real-life systems.[51,56] Fig. 9 shows oscillatory sweep rheograms of 12-6-12/NaBez and 12-6-12/NaBres, where Maxwell behaviour is shown. Comparatively speaking, the elasticity of 12-6-12/NaBez was slightly stronger than that of 12-6-12/NaBres, but the τ_R of both differed significantly since their ω_C values differed by at least one order of magnitude. The longer relaxation time meant more viscous behaviour,[42,57] matching the present situation.

Experimental

Materials

The 12-*s*-12 samples (s = 2, 6, and 10) were synthesised in our laboratory as reported previously.[16] Sodium benzoate (NaBez, AR) and cyclohexane (AR) were purchased from Sinopharm Chemical Reagent Co. (China), sodium salicylate (NaSal, AR) was purchased from J & K Chemical Reagents (China), and sodium 2-bromoethanesulphonate (NaBres, purity ≥ 98.0%) from Acros Organics. All chemicals were used without further purification. The water used was of Milli-Q grade with a resistivity of 18.2 MΩ cm.

Sample preparation

The desired amount of equally charged 12-*s*-12/salt (s = 2, 6, or 10) was mixed in a sample bottle and cyclohexane was added under stirring at 65 °C. The desired amount of water was injected and then the sample was continuously stirred during heating to 75 °C

until the sample became homogeneous. The solutions were kept at 30 °C for at least 12 h to achieve equilibrium.

Methods

Polarised-microscopy observations. Polarised-microscopy observations were conducted on a polarising optical microscope (Olympus BX51TF) equipped with a digital camera (DP12). Samples were prepared by dropping several drops of the solutions onto a thin glass slide, which was then covered by another glass slide.

SAXS measurements. SAXS measurements were performed using a NanoStar (Bruker) SAXS equipped with a 2-d detector. The incident X-rays of CuKα radiation (1.54 Å) were monochromated by a cross-coupled Göbel mirror and passed through the sample placed in a 2 mm quartz capillary. The distance between the sample and the detector was 1070 mm, allowing the value of the scattering vector q to range from 0.07 to 2.3 nm^{-1}. The data shown are for the normalised intensity I (arbitrary units) *versus* $q = (4\pi/\lambda)\sin(\theta)$, where λ represents the wavelength of the X-rays and 2θ is the scattering angle.

Rheological measurements. Rheological measurements were performed on an HAAKE RheoStress 6000 stress-controlled rheometer with a cone-plate sensor. The cone was made of standard ETC steel with a diameter of 60 mm and a cone apex angle of 1°. The gap between the centre of the cone and the plate was 50 μm. Each sample was kept on the plate for 5 min to reach equilibrium before testing. Dynamic frequency-sweep measurements were performed in the linear visco-elastic region of the samples, as determined previously by dynamic stress sweep measurements.

All measurements in this work were carried out at 30 °C.

Fourier transform infrared (FT-IR) measurements. Fourier transform infrared (FT-IR) measurements were performed on a Nicolet iS50 spectrometer (Thermo Fisher Scientic Co., USA) equipped with an ATR detector. Equally charged 12-6-12/NaSal (*s*6/NaSal) was dissolved together in methanol and then the methanol was removed in a drying oven at 50 °C for at least 48 h to obtain an equi-charged mixture of *s*6/NaSal. In addition, desired amounts of equally charged *s*6/NaSal were mixed in sample bottles and the solvents, dimethyl sulfoxide (DMSO) and cyclohexane, were respectively added under stirring. For the DMSO sample, no water was included, and for the cyclohexane sample, a desired amount of water was injected. The samples were continuously stirred at 60 °C (DMSO) and 75 °C (cyclohexane) until they became homogeneous. The FT-IR spectra (4000–400 cm^{-1}) of dried solids of 12-6-12 (*s*6), NaSal and the equi-charged *s*6/NaSal mixture were respectively recorded using KBr pellets at room temperature. The FT-IR spectra of the solution samples were recorded by dropping the sample onto a slide made of diamond in the same scanning range.

Conclusions

The self-assembly of cationic gemini surfactants, 12-*s*-12, together with simple counterions in cyclohexane has been studied. The following conclusions were drawn:

(1) Previously, we reported the preparation of homogeneous samples of 12-*s*-12 in cyclohexane upon addition of a helping surfactant, SH or SL.[16] In the present systems, simple salts were substituted for the helping surfactants, and homogeneous solutions were again achieved. Therefore, it can be expected that the area of self-assembly of ionic gemini surfactants in non-polar solvents will be expanded.

(2) Among the three examined salts, NaSal has a special effect on the construction of complex 12-*s*-12 aggregates due to its *ortho*-hydroxyl in the benzene ring. The NaSal molecule is attracted to the quaternary ammonium head of the 12-*s*-12 favouring intermolecular hydrogen bonding with its neighbouring NaSal molecule. The hydrogen-bonding bridge of water molecules between the NaSal molecules further increased the size of the 12-*s*-12 head. This benefited the formation of aggregates with lower surface curvature.

(3) In a simple salt system, such as NaBes or NaBres, the length of the 12-*s*-12 spacer dominated the associating structure. When NaSal was added, which increased the surfactant head size, two controlling factors (the salt-effect and the spacer-effect) worked in tandem. This not only induced the formation of surfactant aggregates with lower surface curvature, but may also allow the co-existence of multi-type aggregates.

Conflicts of interest

There are no conflicts to declare.

Acknowledgements

Support from the National Natural Science Foundation of China (Grant no 21473032) is gratefully acknowledged.

References

1 P. R. Sundararajan, *J. Polym. Sci., Part B: Polym. Lett.*, 2018, **56**, 451–478.
2 F. Praetorius and H. Dietz, *Science*, 2017, **355**, 1283.
3 M. Komiyama, K. Yoshimoto, M. Sisido and K. Ariga, *Bull. Chem. Soc. Jpn.*, 2017, **90**, 967–1004.
4 M. Mukai and S. Regen, *Bull. Chem. Soc. Jpn.*, 2017, **90**, 1083–1087.
5 N. Liu and T. Liedl, *Chem. Rev.*, 2018, **118**, 3032–3053.
6 Y. Zhao, W. Yang, C. Chen, J. Wang, L. Zhang and H. Xu, *Curr. Opin. Colloid Interface Sci.*, 2018, **35**, 112–123.
7 W. Qi, X. Zhang and H. Wang, *Curr. Opin. Colloid Interface Sci.*, 2018, **35**, 36–41.
8 G. Wang, W. Guan, B. Li and L. Wu, *Curr. Opin. Colloid Interface Sci.*, 2018, **35**, 91–103.
9 M. Huo, Q. Ye, H. Che, X. Wang, Y. Wei and J. Yuan, *Macromolecules*, 2017, **50**, 1126–1133.
10 L. K. Shrestha, R. G. Shrestha, J. P. Hill, T. Tsuruoka, Q. Ji, T. Nishimura and K. Ariga, *Langmuir*, 2016, **32**, 12511–12519.
11 Y. Singh, J. G. Meher, K. Raval, F. A. Khan, M. Chaurasia, N. K. Jain and M. K. Chourasia, *J. Controlled Release*, 2017, **252**, 28–49.

12 M. Molina, M. Asadian-Birjand, J. Balach, J. Bergueiro, E. Miceli and M. Calderón, *Chem. Soc. Rev.*, 2015, **44**, 6161–6186.
13 K. Liu, R. R. Xing, Q. L. Zou, G. H. Ma, H. Möhwald and X. H. Yan, *Angew. Chem., Int. Ed.*, 2016, **55**, 3036–3039.
14 F. M. Menger and C. A. Littau, *J. Am. Chem. Soc.*, 1991, **113**, 1451–1452.
15 R. Zana and J. D. Xia, *Gemini Surfactants*, Marcel Dekker, Inc, New York, 2004 and references therein.
16 S.-L. Deng and J.-X. Zhao, *Soft Matter*, 2018, **14**, 734–741.
17 D.-P. Yang and J.-X. Zhao, *Soft Matter*, 2016, **12**, 4044–4051.
18 G. Yang and J.-X. Zhao, *Rheol. Acta*, 2016, **55**(9), 709–715.
19 C. Rodriguez-Abreu, L. K. Shrestha, D. Varade, K. Aramaki, A. Maestro, A. L. Quintela and C. Solans, *Langmuir*, 2007, **23**, 11007–11014.
20 G. C. Shearman, A. I. I. Tyler, N. J. Brooks, R. H. Templer, O. Ces, R. V. Law and J. M. Seddon, *Liq. Cryst.*, 2010, **37**, 679–694.
21 Y. Zhao, C. Chen and X. Wang, *J. Phys. Chem. B*, 2009, **113**, 2024–2030.
22 I. Martiel, L. Sagalowicz and R. Mezzenga, *Langmuir*, 2013, **29**, 15805–15812.
23 P. Alexandridis, U. Olsson and B. Lindman, *Langmuir*, 1996, **12**, 1419–1422.
24 P. Alexandridis, U. Olsson and B. Lindman, *Langmuir*, 1997, **13**, 23–34.
25 P. Alexandridis, U. Olsson and B. Lindman, *Langmuir*, 1998, **14**, 2627–2638.
26 C. Rodriguez-Abreu, D. P. Acharya, K. Aramaki and H. Kunieda, *Colloids Surf., A*, 2005, **269**, 59–66.
27 M. Pouzot, R. Mezzenga, M. Leser, L. Sagalowicz, S. Guillot and O. Glatter, *Langmuir*, 2007, **23**, 9618–9628.
28 G. Montalvo, M. Valiente and A. Khan, *Langmuir*, 2007, **23**, 10518–10524.
29 Y. Zhao, X. Yue, X. Wang and X. Chen, *J. Colloid Interface Sci.*, 2013, **389**, 199–205.
30 I. W. Hamley, J. A. Pople and O. Diat, *Colloid Polym. Sci.*, 1998, **276**, 446–450.
31 D. Danino, Y. Talmon and R. Zana, *Langmuir*, 1995, **11**, 1448–1456.
32 H. Chung and M. Caffrey, The neutral area surface of the cubic mesophase: location and properties, *Biophys. J.*, 1994, **66**, 377–381.
33 H. Li, L. Dang, S. Yang, J. Li and H. Wei, *Colloids Surf., A*, 2016, **495**, 221–228.
34 Z. Wang, L. Fu, X. Liu, L. Zhang, F. Guo and X. Zhao, *J. Surfactants Deterg.*, 2017, **20**, 673–679.
35 M. J. Pottage, T. Kusuma, I. Grillo, C. J. Garvey, A. D. Stickland and R. F. Tabor, *Soft Matter*, 2014, **10**, 4902–4912.
36 R. F. Tabor, Md. I. Zaveer, R. R. Dagastine, I. Grillo and C. J. Garvey, *Langmuir*, 2013, **29**, 3575–3582.
37 P. Sahoo, N. N. Adarsh, G. E. Chacko, S. R. Raghavan, V. G. Puranik and P. Dastidar, *Langmuir*, 2009, **25**, 8742–8750.
38 J. S. Pedersen, *Adv. Colloid Interface Sci.*, 1997, **70**, 171–210.
39 S. H. Tung, H. Y. Lee and S. R. Raghavan, *J. Am. Chem. Soc.*, 2008, **130**, 8813–8817.
40 H. Y. Lee, K. Hashizaki, K. Diehn and S. R. Raghavan, *Soft Matter*, 2013, **9**, 200–207.
41 H. Li, J. Hao and Z. Wu, *J. Phys. Chem. B*, 2008, **112**, 3705–3710.
42 G. Yang and J.-X. Zhao, *RSC Adv.*, 2016, **6**, 48810–48815.
43 T. S. Banipal, N. Guleriaa, B. S. Lark, P. K. Banipal and G. Singh, *Indian J. Chem.*, 2001, **40A**, 275–282.
44 T. H. Ito, P. C. M. L. Miranda, N. H. Morgon, G. Heerdt, C. A. Dreiss and E. Sabadini, *Langmuir*, 2014, **30**, 11535–11542.
45 V. Lutz-Bueno, S. Isabettini, F. Walker, S. Kuster, M. Liebi and P. Fischer, *Phys. Chem. Chem. Phys.*, 2017, **19**, 21869–21877.
46 L. Zhao, H. Zhang, W. Wang and G. Wang, *J. Mol. Liq.*, 2017, **225**, 897–902.
47 Y. A. Shchipunov and E. V. Shumilina, *Mater. Sci. Eng. C*, 1995, **3**, 43–50.
48 Y. A. Shchipunov, *Colloids Surf., A*, 2001, **183–185**, 541–554.
49 X.-M. Pei, J.-X. Zhao, Y.-Z. Ye, Y. You and X.-L. Wei, *Soft Matter*, 2011, **7**, 2953–2960.
50 D. Philip, A. John, C. Y. Panicker and H. T. Varghese, *Spectrochim. Acta, Part A*, 2001, **57**, 1561–1566.
51 G. Montalvo, M. Valiente and E. Rodenas, *Langmuir*, 1996, **12**, 5202–5208.
52 R. Oda, J. Narayanan, P. A. Hassan, C. Manohar, R. A. Salkar, F. Kern and S. J. Candau, *Langmuir*, 1998, **14**, 4364–4372.
53 D. P. Acharya, H. Kunieda, Y. Shiba and K. Aratani, *J. Phys. Chem. B*, 2004, **108**, 1790–1797.
54 S. Wu, *J. Polym. Sci., Polym. Phys. Ed.*, 1987, **25**, 2511–2529.
55 S. Wu, *J. Polym. Sci., Polym. Phys. Ed.*, 1989, **27**, 723–741.
56 Y. Zhao, X. Yue, X. Wang and X. Chen, *J. Colloid Interface Sci.*, 2013, **389**, 199–205.
57 M. A. Siddig, S. Radiman, L. S. Jan and S. V. Muniandy, *Colloids Surf., A*, 2006, **276**, 15–21.